INTRODUCTION

Neovascular age-related macular degeneration (AMD) is the leading cause of visual loss in elderly in the western world.[1] Photodynamic therapy (PDT) with Verteporfin (Visudyne, Ciba Vision Corp., Duluth, GA) is proved to be beneficial in clinical trials.[2-6] This benefit, however, is limited by high recurrence and high retreatment rate.[2-6] CNV extraction alone is not favored by submacular surgery trials[7] but macular translocation was suggested as an option for patients who did not profit from prior PDT.[8-11] Nevertheless, antiangiogenic therapies[12-14], are now changing the philosophy to a modulative rather than ablative therapy. As adjuvant to PDT, they may increase its efficiency. In order to establish a beneficial combined therapy, it is essential to understand the influence of PDT on the targeted tissue.

Vascular endothelial growth factor (VEGF), a promoter of CNV development,[15,16] is upregulated following verteporfin PDT.[17] Neovascularization, as in CNV, occurs due to an impaired local balance between angiogenesis promoters and inhibitors.[18] VEGF predominates over pigment endothelium derived factor which is an endogeneous angiogenesis inhibitor.[19] Endostatin, a C-terminal fragment of Collagen XVIII, is another potent endogenous angiogenesis inhibitor in CNV.[20,21]

In RPE and choriocapillaris of human eyes with AMD decreased expression of endostatin was suggested to predispose to CNV formation.[22] Laser-induced CNV lesions were significantly bigger in mutant mice lacking Collagen XVIII/Endostatin than in the control animals.[23] Endostatin down-regulates many angiogenic genes including those of VEGF and up-regulates several antiangiogenic genes.[24] Intraocular expression of endostatin reduces VEGF-induced retinal permeability and neovascularization.[25]

In order to understand potential interactions, we evaluated expression and chronological sequence of VEGF, endostatin and E-selectin well as vascularization and proliferative activity in CNV excised after different time intervals following PDT.

METHODS

Subjects and Treatments

We retrospectively reviewed 68 eyes of 68 consecutive AMD patients who were treated with macular translocation at five distinct surgical sites between 1997 and 2005. Twenty-nine patients received surgery after verteporfin PDT. Clinical characteristics of the patients treated with PDT before macular translocation are summarized in Table.

Therapy options, including observation, conventional thermal laser photocoagulation, PDT (re)-treatment, intravitreal triamcinolone injection, macular translocation with 360° retinotomy were discussed with the patients. Surgical intervention was offered when a) visual acuity was below 20/200 being the minimum visual acuity to recommend first PDT according to TAP investigation[2, 3] b) visual deterioration progressed after initial PDT c) patient refused PDT or re-treatment with PDT due to continuous visual deterioration in the fellow eye in spite of PDT and d) PDT was impossible due to recurrent or massive submacular haemorrhage. In four cases, Verteporfin-PDT was performed 3 days prior to surgery with the intention to reduce bleeding from the lesion site at the time of surgical extraction. Three of these cases were not eligible for the first PDT according to TAP criteria as their visual acuity varied between 4/200 and 5/200.[2-6] The fourth patient opted to proceed with surgery rather than PDT re-treatment as he experienced a decrease in visual acuity three months after the first PDT.

Table: Clinical characteristics of patients treated with PDT before surgical removal of the CNV.

Case	Eye	Age/Sex	CNV type	Number of PDT	Time to surgery from the first PDT/Last PDT
1	L	76 / m	Classic	1	3 days
2	R	78 / f	Classic	1	3 days
3	L	54 / m	Pred. Classic	2	113 / 3 days
4	L	84 / m	Classic	1	3 days
5	R	74/f	Occult	1	21 days
6	L	83 / m	Classic	1	34 days
7	L	85 / f	Classic	1	37 days
8	R	73 / f	Occult	3	208/138/40 days
9	L	78 / f	Pred. Classic	2	3 months/ 54 days
10	L	79 / m	Classic	1	55 days
11	R	80 / f	Classic	2	172/69 days
12	L	66 /f	Occult	1	83 days
13	L	77 / m	min. Classic	1	84 days
14	R	79 / f	Pred. Classic	1	88 days
15	L	70/m	Pred Classic	1	92 days
16	R	93 / m	Classic	2	95 days
17	L	76 / f	Occult	1	105 days
18	L	87 / m	Predom. Classic	1	108 days
19	R	71 / m	Classic	1	112 days
20	L	81 / m	Classic	2	213/131 days
21	R	70 / f	Classic	2	151/132 days
22	L	78 / f	Classic	3	344/222/146 days
23	L	77 / m	Classic	3	329/245/147 days
24	L	72 / m	Pred. Classic	2	232/156 days
25	R	79 / f	Pred. Classic	1	171 days
26	R	74 / f	hemorrhagic	1	246 days
27	L	81/f	Classic	6	824/300 days
28	L	73 / f	Classic	4	677/558/467/383 days
29	L	77 / f	Pred. Classic	7	*unknown/772/655 days

CNV = choroidal neovascularization membrane; PDT = photodynamic therapy; m: male, f: female; min: minimally; pred: predominantly, * Time of 1-5th PDT session unknown

Each patient gave written informed consent after the experimental nature of the procedure and risks and benefits of all therapeutical options had been fully explained. The study followed the guidelines of the declaration of Helsinki as revised in Tokyo and Venice. The study and the histological analysis of the specimens were approved by the local Institutional Review Board.

Tissue Preparation

Within minutes after surgery, excised CNV were fixed in 3.7% formalin and subsequently embedded in paraffin. Each specimen was serially mounted on poly-L-lysine coated glass slides (Dako, Glostrup, Denmark).

Immunohistology

Serial sections were de-paraffinized and re-hydrated with a graded series of alcohol. For Cytokeratin 18 and endostatin, antigen retrieval was accomplished by proteolytic digestion with 0.5% protease XXIV (Sigma, St. Louis, MO) whereas Proteinase K (Dako) was used for VEGF. For Ki-67, CD34, CD105 and E-selectin, antigen retrieval was with heat treatment in citrate buffer (0.01 M, ph: 6.0).

Immunohistochemistry with primary antibodies for human CD105 (Mouse, Mab, Clone SN6h, Dako), CD34 (Mouse, Mab, Immunotech, Hamburg, Germany), Ki-67 (Mouse, Mab, Clone Ki-S5, Dako), Cytokeratin 18 (Mouse, Mab, Progen, Heidelberg, Germany) and E-selectin (mouse, Mab, Novocastra, UK) was performed using horseradish peroxidase as previously described.[17] CD34, CD105, cytokeratin 18 and Ki-67 were used to label endothelial cells (EC), activated EC, RPE and proliferating cells, respectively.[26-29]
Immunohistochemistry for VEGF and endostatin were performed by alkaline-phosphatase method as previously described[17] using an anti-human VEGF-A antibody (mouse, Mab, clone C-1; Santa Cruz Biotechnology, Santa Cruz, CA) and an anti-human endostatin antibody (rabbit, polyclonal, Dianova GmbH, Hamburg). Hematoxylin (Chemmate, Code S2020, Dako) was used for counterstaining.
For negative controls, primary antibodies were substituted either by appropriate normal sera or omitted.

Analysis

Serial sections from a specimen were analyzed independently by two masked observers (OT, SG) by light microscopy.

Each specimen was documented with a digital microscope (Axioskop, Zeiss, Oberkochen, FRG) connected to a digital camera (HC-300Z, Fujix, Japan). Area of each specimen was measured using the appropriate hard and software (AxioVision, Version 3.1, Carl Zeiss, Göttingen, Germany).

All Ki-67 positive nuclei all over the section were counted in each specimen. Proliferative activity in a specimen was determined quantitatively by the ratio of the total number of Ki-67 positive nuclei in CNV to the total area of the membrane (mm^2).

Immunoreactivity for VEGF, endostatin and E-selectin were analyzed separately in RPE-Bruch's membrane complex, vessels and stroma. A grading scheme indicating

degree of staining was used. 3,2,1,0 were assigned to indicate intense (70-100% positive cells), moderate (40-69% positive cells), weak labelling (1-39% positive cells) and absence of any staining, respectively. Due to inadequate pre-treatment stability of some sections, E-selectin expression was evaluated in 22 of CNV without PDT and 26 CNV treated with PDT.

"Predominance score of VEGF over endostatin" (PS) was defined for RPE, vessels and stroma of each membrane separately calculating the difference between VEGF and endostatin staining scores.

Intensity of VEGF, endostatin and E-selectin immunostaining, PS and proliferative activity of the defined sub-groups were comparatively analysed with Mann-Whitney U test. $p \leq 0.05$ was considered significant.

RESULTS

Frequency of VEGF, endostatin and E-selectin immunoreactivity intensity and corresponding median staining intensity scores in untreated and PDT treated CNV are summarized in Figure 1.

Characterization of CNV without prior PDT

All but one membrane were vascularized as evidenced by CD34 and CD105 positive vessels (Figures 2A-B). RPE cells were found in all specimens.

Proliferative activity varied between 0-1959.27 Ki-67 positive nuclei/mm^2 (median: 53.6978) (Figure 2C).

VEGF was absent in RPE of 53.8% (21 of 39) of the specimens. In only 12.8% (5 of 39) of the CNV, VEGF was strongly expressed in RPE. VEGF was detected in EC and stromal cells in 60.5% (23 of 38) and 95% (33 of 38) of the membranes, respectively (Figure 1A, 1D, 2D).

Endostatin was found in RPE-Bruch's membrane complex and in vessels in 48.7% (19 of 39) and 76.3% (29 of 38) of the specimens respectively. Within stroma, endostatin was present in fibroblast like and inflammatory cells in 79.5% (31 of 39) of the membranes (Figure 1B, 1D, 2E).

EC, RPE and stromal cells disclosed E-selectin in different intensities in 45.5% (10 of 22), 81.8% (18 of 22), 45.5% (10 of 22) of the membranes, respectively (Figure 1C-D, 2F).

Characterization of CNV treated by PDT

a) Three days after PDT

A hypofluorescence suggesting nonperfusion of the irradiated area and CNV was seen in early phases of angiography (Figure 3A). Late phases of FA revealed hyperfluorescence and leakage at fovea consistent with choroidal ischemia (Data not shown).

Immunohistology with CD34 and CD105 disclosed mostly occluded but several patent vessels lined with damaged EC (Figure 3B).

In all membranes (n=4), cytokeratin18 positive RPE (Figure 3C) displayed an intense staining for VEGF (Figure 1A, 3D) which was significantly higher than in the control group (p=0.0033) (Figure 1D). Endostatin was found in RPE-Bruch's membrane complex of only two membranes (Figure 1B, 3E). Consequently, PS in RPE-Bruch's membrane complex was significantly higher than in the control group (PS =2.5, PS= 0, respectively, p=0.0059).

VEGF expression in EC and stroma varied in intensity (Figure 1A). However, none of the specimens displayed endostatin in vessels or stroma (Figure 1B, 3E). Endostatin expression in vessels and stroma was significantly weaker than control

CNV (Figure 1D, p=0.0366, 0.0028, respectively). Consequently, PS in stroma was significantly higher than in control group (PS=2, PS=0, respectively, p=0.0045).

E-selectin was expressed either in RPE or EC (Figure 1C, 1D, 3F).

Ki-67 was completely negative in 2 cases (median proliferative activity: 4.85505; range: 0-78.758 nuclei/mm^2).

b) post-PDT intervals longer than three days

Fluorescein angiography disclosed hyperfluorescent membranes with leakage in late phases (Data not shown).

Patent vessels lined with CD34 positive EC with prominent nuclei were detected in all but one membrane (Figure 4A). Strong CD105 immunoreactivity reflected very vital and active EC. Some CD105 negative EC were also detected (Figure 4B). VEGF was detected in EC in 21 (87%) samples (Figure 4C). Vessels displayed endostatin in 82.8% (19 of 24) of CNV (40%) in a stronger intensity than in CNV extracted 3 days after PDT (p=0.0073) (Figure 1B,1D, 4D-E). E-selectin was seen in EC in 50% (11 of 22) of the specimens (Figure 1C, Figure 4F-G).

All but one membrane (Case 17 in Table) were extracted with RPE as evidenced by cytokeratin18 staining. Strong VEGF staining in RPE in 66.7% (16 of 24) (Figure 1A and 4C) of the specimens persisted to be significantly higher than in the control group (Figure 1D, p<0.0001). Endostatin expression in RPE (in 23 of 24) was significantly higher (Figure 1B, 4D-E, p=0.0257), and consequently, PS in RPE was significantly lower than in CNV extracted three days after PDT (Figure 1D, PS=0, PS=2.5, p=0.0017, respectively). RPE expressed E-selectin in 47.8% (11 of 23) of the specimens (Figure 1C, 4F-G)

Stromal cells displayed VEGF and endostatin in 92% (23 of 25) of membranes (Figure 1A, 1B, 4C-E). Endostatin in stroma was considerably stronger (Figure 1D, p=0.0015) and PS in stroma (PS=0) was significantly lower than in CNV treated by PDT three days preoperatively (PS=2) (p=0.0152). Stromal cells disclosed E-selectin in 26.1% (6 of 23) of the specimens (Figure 1C, 4F-G).

No significant change was found in pattern of E-selectin expression in any component of the CNV subgroups examined.

Proliferative activity (median: 114.125, range: 0-955.235) was significantly higher than both CNV extracted 3 days after PDT (p=0.0227) and control group (p=0.0204) (Figure 4H).

DISCUSSION

PDT is based on the formation of free radicals and reactive oxygen intermediates (ROI) which damage EC and lead to a selective occlusion of the targeted vessels.[30-32] In more than 90% of the cases, however, a recurrence is seen within 3 months.[2-6] Enhanced VEGF expression[17] and predominance over PEDF[19] might contribute to this rebound effect. Herein, we investigated the potential involvement of E-selectin and endostatin within this process.

E-selectin is a prerequisite for the anti-angiogenic effect of endostatin.[33] Similar to a previous study,[34] we did not see a significant change in E-selectin expression following PDT.

In contrast, endostatin was significantly weaker in intensity in vessels and stroma three days after PDT compared to the untreated specimens. As a consequence, VEGF predominates over endostatin in RPE-Bruch's membrane and stroma early after PDT. A hypoperfusion related hypoxia as well as the release of ROI after PDT may have up regulated VEGF expression by RPE.[35-41] To our knowledge, impact of PDT and hypoxia on ocular endostatin expression is unknown. Reduction of endostatin, however, was suggested to play an active role in hypoxia driven angiogenesis elsewhere.[42,43]

Endostatin has important implications in inhibition of angiogenesis and ischemia-induced neovascularization.[44] In early phases of angiogenesis, it inhibits VEGF induced EC migration, stabilizes newly formed endothelial tubes,[45,46] downregulates VEGF expression and blocks VEGF/Flk-1 pathway.[47,48] Decreased levels of endostatin with consequent VEGF predominance three days after PDT may, therefore, play a permissive role in the reactive angiogenic process.

In CNV extracted at longer time intervals after PDT, endostatin expression was significantly enhanced in RPE-Bruch's membrane, EC and stroma. Zatterstrom et al suggested that activated EC secrete proteolytic enzymes[49] which release active endostatin from Collagen XVIII in vascular basement membranes.[50] This might explain that endostatin was diminished in early post-PDT period when EC were severely damaged[30-32] but enhanced thereafter when healthy EC were found. Increased infiltration with leukocytes (unpublished data) producing proteolytic enzymes may also contribute to enhanced release of endostatin.[51] As a consequence, VEGF predominance over endostatin is diminished or abolished at a certain phase of the revascularization process after PDT. High proliferative activity, patent vessels with activated EC and persisting leakage in fluorescein angiography in these specimens appear paradoxical, but may be the result of the previous disbalance with VEGF predominance. It has been previously shown that even temporary enhanced VEGF expression by RPE was sufficient for increased vascular leakage and development of CNV.[52] Therefore, insufficient counterbalance of VEGF early after PDT seems to have restarted the angiogenic cascade. Inhibition of vessel growth by endostatin would have required an early and substantial presence of endostatin.[53,54]

Endostatin inhibits experimental CNV [55-57] and its expression can be up-regulated by orally administered drugs.[58] Up-regulation or exogeneous delivery of endostatin early after PDT might be therefore a useful strategy to increase efficacy of PDT. A

concomitant anti-VEGF therapy, having a synergistic effect[59,60] should be even more potent.

The sequence of histopathological changes in CNV after PDT is probably reflecting not the cause but the natural process of CNV formation. Enhanced endostatin expression in late stages of angiogenesis possibly contributes to the involution process. The exact time of CNV onset is mostly unknown and the age of the membranes at the time of PDT and/or surgery can not be assessed. PDT, however, gives an artificial but accurate "time zero" that enables a chronological analysis of the revascularisation process and the humoral and cellular mechanisms involved. An absolute quantification of the mRNA and/or protein expression by real time PCR and/or western blot in further studies will probably supply additional valuable information.

To our knowledge, it is the first report of clinicopathological correlation related to the expression of endostatin in human CNV treated by verteporfin PDT. The proper interpretation of this study is limited by a potential negative selection of PDT treated cases based on the retrospective and non-randomized characteristics. Additionally, the maturity and angiogenic activity of the specimens probably vary within and between groups and can not be unified precisely. Nevertheless, our findings reveal that angiogenic VEGF predominates over antiangiogenic endostatin early after PDT. An exogenous or endogenous increase of endostatin in this phase is a potential approach that merits investigation.

Grant support: Vision 100 Foundation
Commercial relationship: none

REFERENCES

1) Ambati J, Ambati BK, Yoo SH, Ianchulev S, Adamis AP. Age-related macular degeneration: etiology, pathogenesis, and therapeutic strategies. Surv Ophthalmol 2003;48:257-93.
2) Treatment of Age-Related Macular Degeneration with Photodynamic Therapy (TAP) Study Group. Photodynamic therapy of subfoveal choroidal neovascularization in age-related macular degeneration with verteporfin: one-year results of 2 randomized clinical trials—TAP Report 1. Arch Ophthalmol 1999;117:1329-1345.
3) Treatment of Age-Related Macular Degeneration with Photodynamic Therapy (TAP) Study Group. Photodynamic therapy of subfoveal choroidal neovascularization in age-related macular degeneration with verteporfin: two-year results of 2 randomized clinical trials—TAP Report 2. Arch Ophthalmol 2001;119:198-207.
4) Treatment of Age-Related Macular Degeneration with Photodynamic Therapy (TAP) Study Group. Verteporfin therapy of subfoveal choroidal neovascularization in patients with age-related macular degeneration: additional information regarding baseline lesion composition's impact on vision outcomes-TAP report No. 3. Arch Ophthalmol 2002;120:1443-54.
5) Verteporfin in Photodynamic Therapy Study group. Verteporfin therapy of subfoveal choroidal neovascularization in age-related macular degeneration: two-year results of a randomized clinical trial including lesions with occult with no classic choroidal neovascularization—Verteporfin in Photodynamic Therapy report 2. Am J Ophthalmol 2001;131:541-560.
6) Blinder KJ, Bradley S, Bressler NM,et al; Treatment of Age-related Macular Degeneration with Photodynamic Therapy study group; Verteporfin in Photodynamic Therapy study group. Effect of lesion size, visual acuity, and lesion composition on visual acuity change with and without verteporfin therapy for choroidal neovascularization secondary to age-related macular degeneration:TAP and VIP report no. 1. Am J Ophthalmol 2003;136:407-18.
7) Hawkins BS, Bressler NM, Miskala PH, et al. Submacular Surgery Trials (SST) Research Group. Surgery for Subfoveal Choroidal Neovascularization in Age-Related Macular Degeneration: Ophthalmic Findings SST Report No. 11 Ophthalmology 2004;111:1967–1980.
8) Park CH, Toth CA. Macular translocation surgery with 360-degree peripheral retinectomy following ocular photodynamic therapy of choroidal neovascularization. Am J Ophthalmol 2003;136:830-5.
9) Mirshahi A, Schreyger F, Baatz H, et al. Macular translocation after photodynamic therapy: a case report. Klin Monatsbl Augenheilkd 2005;222:586-9.
10) Fujii GY, de Juan E Jr, Humayun MS, Chang TS. Limited macular translocation for the management of subfoveal choroidal neovascularization after photodynamic therapy. Am J Ophthalmol. 2003;135(1):109-12.
11) Glacet-Bernard A, Coscas G, Soubrane G. Pigment epithelial changes in young women treated with photodynamic therapy and limited macular translocation for classic choroidal neovascularisation. Graefes Arch Clin Exp Ophthalmol. 2006 Mar 8; [Epub ahead of print]
12) Gragoudas ES, Adamis AP, Cunningham ET Jr, Feinsod M, Guyer DR; VEGF Inhibition Study in Ocular Neovascularization Clinical Trial Group. Pegaptanib

for neovascular age-related macular degeneration. N Engl J Med 2004;351:2805-16.
13) Avery RL, Pieramici DJ, Rabena MD, Castellarin AA, Nasir MA, Giust MJ. Intravitreal Bevacizumab (Avastin) for Neovascular Age-Related Macular Degeneration. Ophthalmology 2006;113:363-372.
14) Campochiaro PA, Nguyen QD, Shah SM, et al. Adenoviral Vector-Delivered Pigment Epithelium-Derived Factor for Neovascular Age-Related Macular Degeneration: Results of a Phase I Clinical Trial. Hum Gene Ther 2006;17:167–176.
15) Kwak N, Okamoto N, Wood J, Campochiaro P. VEGF is major stimulator in model of choroidal neovascularization. Invest Ophthalmol Vis Sci 2000;41:3158-3164.
16) Baffi J, Bymes G, Chan CC, Csaky KG. Choroidal neovascularization in the rat induced by adenovirus mediated expression of vascular endothelial growth factor. Invest Ophthalmol Vis Sci 2000;41:3582-9.
17) Tatar O, Kaiserling E, Adam A, et al. Consequences of Verteporfin Photodynamic Therapy on Choroidal Neovascular Membranes. Arch Ophthalmol 2006; 124:815-23.
18) Hanahan D, Folkman J. Patterns and emerging mechanisms of the angiogenic switch during tumorigenesis. Cell. 1996;86:353-64.
19) Tatar O, Adam A, Shinoda K, et al. Expression of VEGF and PEDF in choroidal neovascular membranes following verteporfin photodynamic therapy. Am J Ophthalmol. 2006;142:95-104.
20) ÕReilly MS, Boehm T, Shing Y, et al. Endostatin: an endogenous inhibitor of angiogenesis and tumor growth. Cell 1997;88:277-285.
21) Tatar O, Shinoda K, Adam A, et al. Expression of Endostatin in Human Choroidal Neovascular Membranes secondary to Age-related Macular degeneration. Exp Eye Res 2006; 83:329-38. Epub 2006 Apr 11.
22) Bhutto IA, Kim SY, McLeod DS, et al. Localization of Collagen XVIII and the Endostatin Portion of Collagen XVIII in Aged Human Control Eyes and Eyes with Age-Related Macular Degeneration. Invest Ophthalmol Vis Sci 2004;45:1544-1552.
23) Marneros AG, Zambarakji H, She H, et al. Increased Laser–Induced Choroidal Neovascularization in Mice Lacking Collagen XVIII/Endostatin. Invest. Ophthalmol. Vis. Sci. 2006 47: E-Abstract 1532.
24) Abdollahi A, Hahnfeldt P, Maercker C, et al. Endostatin's Antiangiogenic Signaling Network. Mol Cell 2004;13:649-63.
25) Takahashi K, Saishin Y, Saishin Y, et al. Intraocular expression of endostatin reduces VEGF-induced retinal vascular permeability, neovascularization, and retinal detachment. FASEB J 2003;17:896-8.
26) Sasano H, Suzuki T. Pathological evaluation of angiogenesis in human tumor. Biomed Pharmacother. 2005;59 Suppl 2:S334-6.
27) Yasukawa T, Kimura H, Tabata Y, et al. Active drug targeting with immunoconjugates to choroidal neovascularization. Curr Eye Res 2000;21:952-61.
28) Grossniklaus HE, Ling JX, Wallace TM, et al. Macrophage and retinal pigment epithelium expression of angiogenic cytokines in choroidal neovascularization. Mol Vis 2002;8:119-26.
29) Karak AK, Sarkar C, Chumber S, Tandon N. MIB-1 proliferative index in parathyroid adenoma and hyperplasia. Indian J Med Res 1997; 105:235-238.

30) Grisanti S, Tatar O, Canbek S, et al. Immunohistopathologic evaluation of choroidal neovascular membranes following Verteporfin-Photodynamic Therapy. Am J Ophthalmol 2004;137: 914-923.
31) Schmidt-Erfurth U, Hasan T. Mechanisms of action of photodynamic therapy with verteporfin for the treatment of age-related macular degeneration. Surv Ophthalmol 2000;45:195-214.
32) Petermeier K, Tatar O, Inhoffen W, et al. Verteporfin photodynamic therapy induced apoptosis in choroidal neovascular membranes. Br J Ophthalmol. 2006;90:1034-9. Epub 2006 Apr 13.
33) Yu Y, Moulton KS, Khan MK, et al. E-selectin is required for the antiangiogenic activity of endostatin. Proc. Natl. Acad. Sci U. S. A. 2004;101:8005-8010.
34) Yeh DC, Bula DV, Miller JW, Gragoudas ES, Arroyo JG. Expression of leukocyte adhesion molecules in human subfoveal choroidal neovascular membranes treated with and without photodynamic therapy. Invest. Ophthalmol. Vis. Sci 2004;45, 2368-73.
35) Schmidt-Erfurth U, Michels S. Changes in confocal indocyanine green angiography through two years after photodynamic therapy with verteporfin. Ophthalmology 2003;110,1306-1314.
36) Michels S, Schmidt-Erfurth U. Sequence of early vascular events after photodynamic therapy. Invest Ophthalmol Vis Sci 2003;44:2147-54.
37) Michels S, Hansmann F, Geitzenauer W, Schmidt-Erfurth U. Influence of Treatment Parameters on Selectivity of Verteporfin Therapy. Invest Ophthalmol Vis Sci 2006;47:371-76.
38) Schlingemann RO. Role of growth factors and the wound healing response in age-related macular degeneration. Graefes Arch Clin Exp Ophthalmol 2004;242:91-101.
39) Shima DT, Adamis AP, Ferrara N, et al. Hypoxic induction of endothelial cell growth factors in retinal cells: Identification and characterization of vascular endothelial growth factor (VEGF) as the mitogen. Mol Med 1995;1:182-193.
40) Shima DT, Deutsch U, D'Amore PA. Hypoxic induction of vascular endothelial growth factor (VEGF) in human epithelial cells is mediated by increases in mRNA stability. FEBS Lett 1995;370:203-8.
41) Kuroki M, Voest EE, Amano S, et al. Reactive oxygen intermediates increase vascular endothelial growth factor expression in vitro and in vivo. J Clin Invest 1996; 98: 1667-75.
42) Wu P, Yonekura H, Li H, et al. Hypoxia down-regulates endostatin production by human microvascular endothelial cells and pericytes. Biochem Biophys Res Commun 2001; 288: 1149-54.
43) Nasu K, Nishida M, Fukuda J, Kawano Y, Nishida Y, Miyakawa I. Hypoxia simultaneously inhibits endostatin production and stimulates vascular endothelial growth factor production by cultured human endometrial stromal cells. Fertil Steril 2004;82:756-9.
44) Dobryansky M, Galiano RD, Cetrulo CL Jr, et al. Endostatin inhibits ischemia-induced neovascularization and increases ischemic tissue loss. Ann Plast Surg 2004;52:512-8
45) Eriksson K, Magnusson P, Dixelius J, Claesson-Welsh L, Cross MJ. Angiostatin and endostatin inhibit endothelial cell migration in response to FGF and VEGF without interfering with specific intracellular signal transduction pathways FEBS Lett 2003;536:19-24.

46) Ergun S, Kilic N, Wurmbach JH, et al. Endostatin inhibits angiogenesis by stabilization of newly formed endothelial tubes. Angiogenesis 2001;4:193-206.
47) Hajitou A, Grignet C, Devy L, et al. The antitumoral effect of endostatin and angiostatin is associated with a down-regulation of vascular endothelial growth factor expression in tumor cells. FASEB J 2002;16:1802-4.
48) Jia YH, Dong XS, Wang XS. Effects of endostatin on expression of vascular endothelial growth factor and its receptors and neovascularization in colonic carcinoma implanted in nude mice. World J Gastroenterol 2004;10:3361-4.
49) Zatterstrom UK, Felbor U, Fukai N, Olsen BR. Collagen XVIII/endostatin structure and functional role in angiogenesis. Cell Struct Funct 2000;25:97-101.
50) Ferreras M, Felbor U, Lenhard T, Olsen BR, Delaisse J. Generation and degradation of human endostatin proteins by various proteinases. FEBS Lett 2000;486, 247–251.
51) Sunderkotter C, Steinbrink K, Goebeler M, Bhardwaj R, Sorg C. Macrophages and angiogenesis. J Leukoc Biol 1994;55:410-22.
52) Spilsbury K, Garrett KL, Shen WY, et al. Overexpression of Vascular Endothelial Growth Factor (VEGF) in the Retinal Pigment Epithelium Leads to the Development of Choroidal Neovascularization. Am J Pathol 2000;157:135-144.
53) Macpherson GR, Ng SSW, Forbes SL, et al. Anti-angiogenic activity of endostatin is HIF-1- is independent and sensitive to timing of treatment in a human sapheneous vein assay. Mol Cancer Ther 2003;2:845-854.
54) Fukai N, Eklund L, Marneros AG, et al. Lack of collagen XVIII/endostatin results in eye abnormalities. EMBO J 2002; 21, 1535-1544.
55) Mori K, Ando A, Gehlbach P, et al. Inhibition of choroidal neovascularization by intravenous injection of adenoviral vectors expressing secretable endostatin. Am J Pathol 2001 ;159:313-20.
56) Shang QL, Ma JX, Wei JS, Shang ZL, Xiu HM, Yang AQ. Experimental choroidal neovascularization is inhibited by subretinal administration of Endostatin. Zhonghua Yan Ke Za Zhi 2004;40:266-71.
57) Balaggan KS, Binley K, Esapa M, et al. EIAV vector-mediated delivery of endostatin or angiostatin inhibits angiogenesis and vascular hyperpermeability in experimental CNV. Gene Ther. 2006;13:1153-65. Epub 2006 Jun 13.
58) Folkman J. Endogeneous angiogenesis inhibitors. APMIS. 2004;112:496-507.
59) Abdollahi A, Lipson KE, Sckell A, et al. Combined therapy with direct and indirect angiogenesis inhibition results in enhanced antiangiogenic and antitumor effects Cancer Res. 2003;63:8890-8.
60) Pan X, Wang Y, Zhang M, Pan W, Qi ZT, Cao GW. Effects of endostatin-vascular endothelial growth inhibitor chimeric recombinant adenoviruses on antiangiogenesis. World J Gastroenterol 2004;10:1409-14.

Figure 1: Graphs showing VEGF (A), endostatin (B) and E-selectin (C) immunostaining intensity and median staining intensity scores (D) in CNV without PDT and CNV extracted 3 days and longer than 20 days after PDT. VEGF, endostatin, and E-selectin immunostaining in retinal pigment epithelium (RPE)-Bruch's membrane, vessels and stromal cells were evaluated separately and semiquantitatively as intense (70-100% positive cells), moderate (40-69% positive cells), mild (1-39% positive cells) or absent. Staining scores of 3,2,1,0 were assigned to "intense", "moderate", "mild" and "absent" intensity of staining, respectively.

Figure 2: Photomicrographs of a surgically excised CNV without prior PDT. The specimens were probed with antibody against CD34 (A), CD105 (B), Ki-67 (C) stained with 3-Diaminobenzidine resulting in a brown chromogen; VEGF (D) and endostatin (E) stained with red chromogen; and E-selectin (F) with AEC. Hematoxylin was used as counterstain. CD34 (A) and activated endothelial cell marker CD105 (B) are selectively expressed in vascular structures (arrow). The brown chromogen can be distinguished from the melanin granula (asterisk) contained in pigmented cells. Several cell nuclei express the proliferation marker Ki-67 (C, arrow). In the serial section of the same specimen (D), VEGF staining was detected within endothelial cells (arrow) and stromal cells (white arrow). In a serial section probed with endostatin, RPE-Bruch's membrane (asterisks) and vessels (arrow) express endostatin (E). (F) Some RPE cells (asterisk) display E-selectin immunoreactivity whereas some RPE cells are not immunoreactive (white arrow head). Scale bar: 50 µm.

Figure 3: Photomicrographs of CNV membrane (case 4, Table 1), extracted 3 days after PDT. Early phase of fluorescein angiography (A) on the day of surgery displays nonperfusion of the CNV and laser spot area. The serial sections were probed with CD34 (B), cytokeratin 18 (C), VEGF (D), endostatin (E) and E-selectin (F). Some vessels depicted by the brown chromogen are patent but still lined with damaged endothelial cells (B, arrow). Retina pigment epithelium (C, asterisks) are strong positive for VEGF (D, asterisks) but not immunoreactive for endostatin (E, asterisk). Endostatin immunoreactivity is absent in CNV (E). Endothelial cells express E-selectin (F, arrows). Scale bar: 50 µm.

Figure 4: Photomicrographs of CNV membranes extracted 55 and 383 days after PDT from Case 10 (A-D, F, H) and Case 28 (E, G) in Table. The sections were probed with CD34 (A), CD105 (B), VEGF (C), endostatin (D, E), E-selectin (F, G) and Ki-67 (H). Most of the vessels depicted by the brown chromogen are patent and lined with healthy activated endothelial cells (A, B, arrows). The brown chromogen can be distinguished from the melanin granula (asterisk) contained in pigmented cells. (C) RPE (asterisk), endothelial cells (arrows) and stromal cells (white arrow) display VEGF (red chromogen) strongly. (D, E) Endostatin expression becomes stronger in RPE-Bruch's membrane complex (asterisk), vessels (arrows) and stromal cells (white arrow) as time interval following PDT increases. (F, G) Endothelial cells (arrows), some stromal cells (white arrow) and some RPE cells (asterisk) express E-selectin whereas some RPE cells are E-selectin negative (white arrow head). (H) Many Ki-67 expressing proliferating cells were detected in the serial section of the CNV from Case 10 (arrows, brown chromogen). Scale bar: 50 µm.

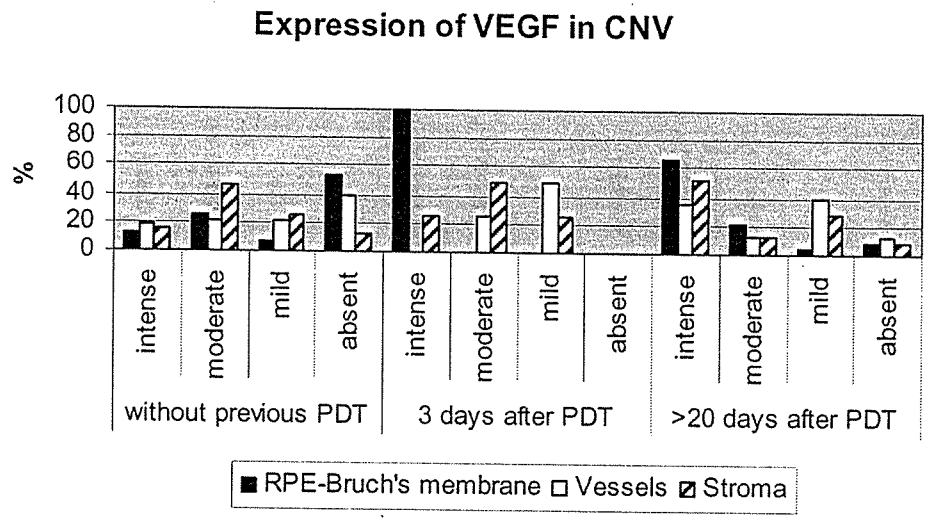
Expression of VEGF in CNV
100
80
60
40
20
0
%
intense
moderate
mild
absent
intense
moderate
mild
absent
intense
moderate
mild
absent
without previous PDT
3 days after PDT
>20 days after PDT
RPE-Bruch's membrane
Vessels
Stroma

Expression of Endostatin in CNV

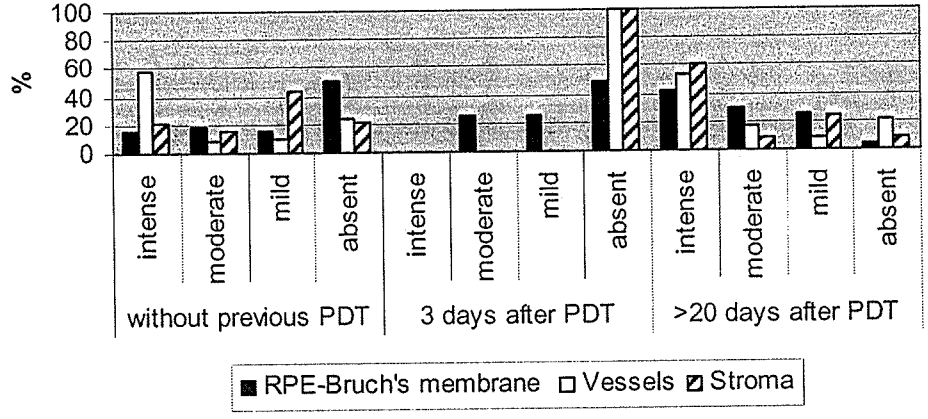

Expression of E-selectin in CNV

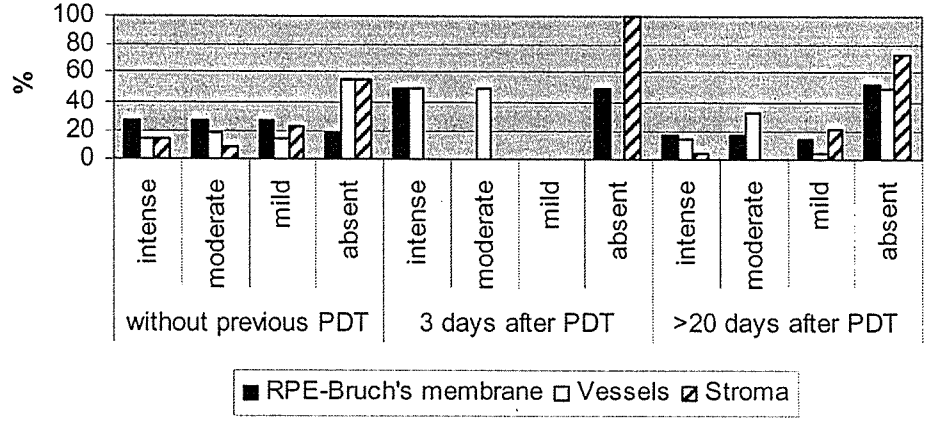

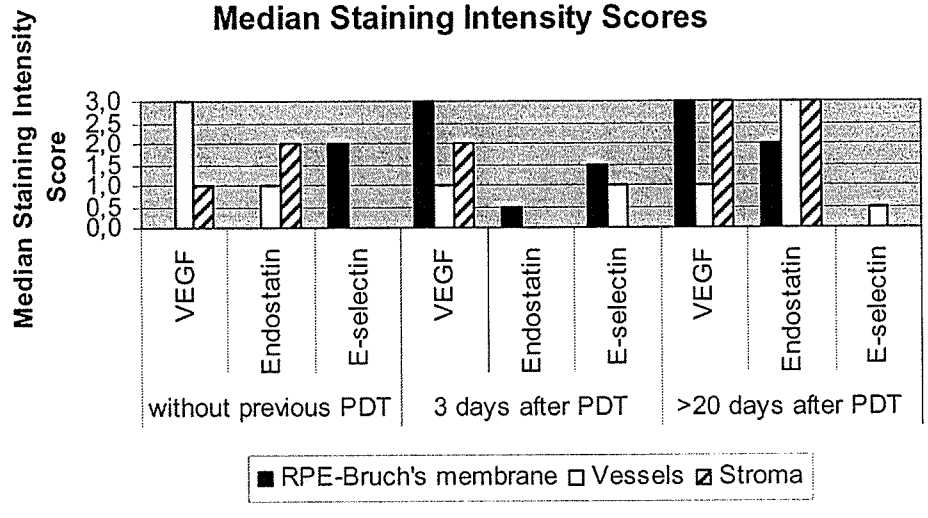
Median Staining Intensity Scores
Median Staining Intensity Score
3,0
2,5
2,0
1,5
1,0
0,5
0,0
VEGF
Endostatin
E-selectin
VEGF
Endostatin
E-selectin
VEGF
Endostatin
E-selectin
without previous PDT
3 days after PDT
>20 days after PDT
RPE-Bruch's membrane
Vessels
Stroma

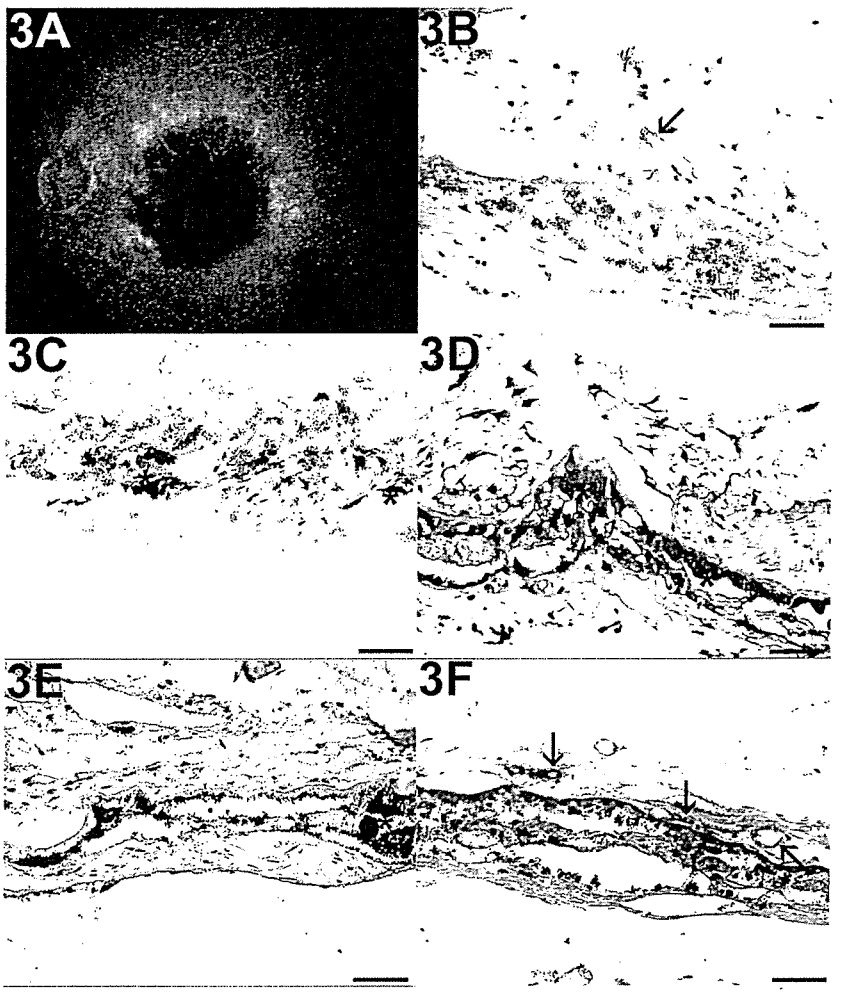
3A
3B
3C
3D
3E
3F